

Control of a decelerating boundary layer. Comparison of different actuators using PIV.

Michel Stanislas

Laboratoire de Mécanique de Lille, France
Bv Paul Langevin, cité Scientifique
59655 Villeneuve d'Ascq France
stanislas@ec-lille.fr

Gilles Godard

CNRS UMR 6614 - CORIA
76801 Saint Etienne du Rouvray cedex
gilles.godard@coria.fr

ABSTRACT

The control of boundary layer separation on the suction side of an airfoil at high angle of attack has been renewed by the possibilities of active control. Nevertheless, such an active control needs a deep understanding of the flow to manipulate and of the actuating flow, both being 3D and unsteady. For that purpose, a model experiment has been designed in the frame of a coordinated European project called AEROMEMS, with a simple (2D) geometry and with a dilatation of the scales in order to be able to characterize the actuation flow. This model is a bump in a boundary layer wind tunnel, which mimics the adverse pressure gradient on the suction side of an airfoil at the verge of separation. The present contribution describes tests performed in the frame of the AEROMEMS II project to compare standard passive devices with active jets systems. The optimization was done with hot film shear stress probes, the characterization with PIV. The results show quantitatively the improvement brought by the devices in terms of skin friction. They also show the mechanism which is at the origin of this improvement.

INTRODUCTION

The control of separation is one of the leading problems in fluid engineering. Flow control can be used for many technological applications to increase performances by “(1) delaying/advancing boundary layer transition, (2) suppressing/enhancing turbulence and (3) preventing excessive boundary layer growth and separation”. Numerous control mechanisms have been tested and can be implemented from the leading edge, down to the trailing edge of an airfoil. In a recent paper, Stanewsky (2001) has reviewed different boundary layer active (and passive) control techniques. For the control of a boundary layer, each type of problem requires a specific solution :

- Turbulent transition can be controlled with adaptive wing elements pneumatically activated in a periodic manner at a chosen frequency (vibrating surface; suction/blowing airflow devices),
- Laminar flow control can be done by leading edge suction,
- Reduction of skin-friction drag is possible when acting on near wall structure by surface air injection or by interactive actuator and sensor arrangement,
- Lift enhancement and separation suppression can be induced by longitudinal vortices (at the scale of the BL thickness), generated by pulsed or continuous jets.

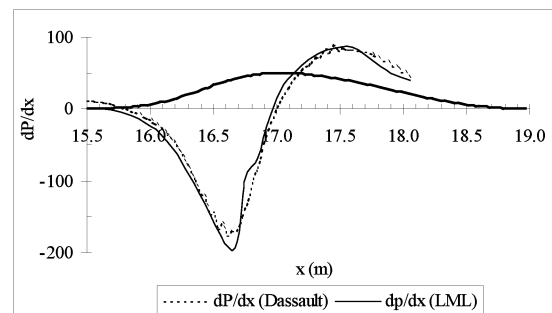


Figure 1: Comparison of experimental and numerical pressure gradient on the bump ($U_{inf} = 8.72$ m/s).

In the AEROMEMS project, the generation, at a substantial distance upstream of the separation point, of streamwise near wall coherent structures was studied, in order to increase the skin friction in adverse pressure gradient condition (Bernard & al (2000)). For that purpose, experiments were performed in a Boundary Layer wind tunnel. A two-dimensional bump, which mimics the longitudinal adverse pressure gradient on the suction side of an airfoil at the verge of separation, was designed, fabricated and mounted in the test section. The flow was explored, with and without actuation by means of hot wire anemometry, skin friction measurements and

PIV. Some basic configurations of actuator devices were tested and their direct influence on the flow was characterized. An array of passive devices, was shown to generate a significant increase in skin friction by generating strong streamwise vortices in the boundary layer. Subsequently different pulsed jets through slots were tested. The better results were obtained with an array of double slotted jets placed at an angle of 45° between the slots and the streamwise direction.

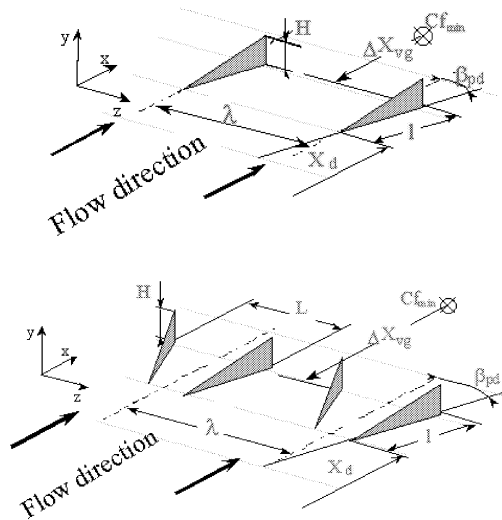


Figure 2: Counter rotating passive device configuration.

AEROMEMS II is the continuation of the previous AEROMEMS project. After the slots device definition it was necessary to perform an extensive parametric study in order to try to limit the velocity ratio. Apart for the location on the bump, it was possible to test a full range of geometrical parameters, of flow velocity ratios (VRe) and of pulsating frequency. Due to the difficulty to evaluate directly the capability of a system optimized in the present experimental configuration to prevent separation on a real airfoil, it was decided to use a system well described in the literature as reference. Attention was focused on vane type longitudinal Vortex Generators (VGs). This technology, first introduced by Taylor in 1947, is well known today (Rao (1988), Pauley (1988), Lin (1989-2002), Betterton. (2000), Jenkins (2002), Angele (2003) ...). In a first step, an optimisation of this type of passive devices on the LML bump and a parametric study of the AEROMEMS slots configuration led to the conclusion that the slots are less effective than the passive vane type VGs. In a second step, different configurations were looked for to find and optimize an active system that produces at least the vane type VGs skin friction increases. Based on longitudinal vortex generation, the pitch and skewed round jet actuators were chosen. This technology seems to have the most important background and to present the highest degree of accessibility in term of defining, validating and integrating it into a real structure. With the same approach as for the slots devices, a new parametric study based on existing literature was performed. Finally, a stereo PIV test campaign was performed in three planes normal to the flow in order to characterize the actuating flow for the best configurations.

EXPERIMENTAL SET-UP

For the present experiments, the same boundary layer wind tunnel as in Bernard & al (2003) was used (see this reference for a detailed description). The test section is $1 \times 2 \text{ m}^2$ and 20 m long. The last 5 m are transparent on all sides to allow the use of optical methods. The free stream velocity can be varied continuously from 1 to 10 m/s but was fixed here at 8.72 m/s. The flow without control was previously characterized in detail by Bernard & al (2003). Figure 1 gives the pressure gradient along the bump which shows that the flow is strongly accelerating in the first half of the bump with a rapid variation of the pressure gradient magnitude and then decelerating in the second half. In this region, both pressure gradient and curvature affects the flow. This is fairly representative of what happens on the suction side of an airfoil at moderately high angle of attack.

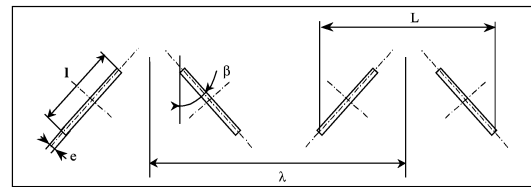


Figure 3 : Counter rotating slot device configuration.

In order to obtain a significant 2D adverse pressure gradient in the wind tunnel, the bump was designed and manufactured in the AEROMEMS project. The shape was computed by Dassault Aviation, using a two-dimensional Navier-Stokes solver with a $k-\epsilon$ turbulence model. The objective was to approach separation without reaching it in order to prevent the flow to become three-dimensional. The 2D bump is attached on the wind tunnel floor.

Based on the literature results, only one type of passive actuator was tested in the present study. This is the thin plate triangular vortex generator as suggested by Lin (1999) and as illustrated in figure 2. For the active devices, slotted jets, as illustrated by figure 3 and round jets as in figure 4, were tested.

In order to obtain quickly a quantitative information on the efficiency of each configuration tested, the wall shear stress was measured with hot film probes. These measurements were performed mainly at the location of minimum shear stress of the smooth configuration. Senflex SF9902 hot film probes were used for that purpose coupled to an AALAB AN1003 anemometer.

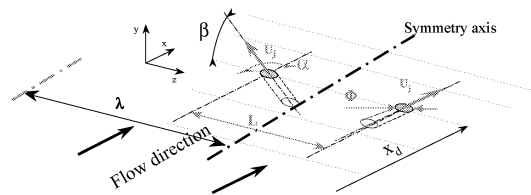


Figure 4: Counter-rotating round jets vortex generators configuration.

A standard stereo PIV set-up was used in this experiment. The laser system allowed to obtain two pulses of about 600 mJ each. As the main flow was going through the light sheet, a small separation, of the order of

Table 1: Optimal parameters for both configurations of passive devices.

	VGs	h/δ	ΔXvg/h	l/h	L/h	λ/h	β _{pd} (°)	Δτ/τ ₀ (%)	
								min	max
CtR	Triangular Vanes	0.37	57	2	2.5	6	18	110	200
CoR	Triangular Vanes	0.37	57	2	-	6	18	55	105

Table 3: Optimal parameters for round jets devices.

VGs	α (°)	β (°)	Φ/δ	λ/Φ	L/Φ	VR _e	Δτ/τ ₀ (%)
							max
CtR	45-90	45	0.036	-	15	≥ 3.1	200
CoR	45-90	45	0.036	6	-	4.7	220

0.5 mm was set between the first and the second pulse of the laser system, to allow a larger dynamic range. At each measurement station, the light sheet, which comes in the wind tunnel through the side wall, was set normal to the bump wall. To record the images, two PCO SensiCam cameras from Lavision were used. They acquire 1280x1024 pixels image pairs and provide a 12 bits dynamic range. Special mounts were used to set the cameras in the Sheimpflug conditions. Nikon lenses of focal length $f = 200$ mm were used. The magnification was around $M = 0.14$. With an aperture of $f\# = 4$ the diffraction spot size was of the order of $20 \mu\text{m}$. The calibration was performed by recording images of a plane target at 3 different positions in depth.

The image processing was performed using a homemade software. The images from both cameras were processed with a standard multigrid algorithm with discrete window shifting. The final interrogation window size was 32×32 pixels with 50% of overlap. This gives 5336, 4292 and 4275 vectors respectively in the three planes investigated. The Soloff method with 3 calibration planes (Soloff (1997)) was used to reconstruct the three velocity components in the plane of measurement. This was done using a home made software.

Table 2 : Counter-rotating slots, optimal configuration.

VR	e/l	L/δ	L/l	λ/l	β(°)	Δτ/τ (%)
6	1/15	0.099	2.08	6.87	15	70/55

RESULTS

Optimization

The first part of the study did consist in testing and optimizing the different actuators by means of skin friction measurement. These comparative measurements were obtained at the streamwise location $X_{cfmin} = 18.58$ m, where the skin friction coefficient C_f reaches a minimum on the smooth wall. The procedure used

allowed to get a quantitative assessment of the skin friction variation due to the actuation. For these counter-rotating devices, the length L , height h , spacing λ , angle β and streamwise position Xvg of the actuators were varied (see figure 2). For the co-rotating actuators, only the spacing was optimized, the other parameters were taken from the optimal counter-rotating configuration. Table 1 gives the resulting optimal configuration for both situations. The smooth boundary layer thickness is δ at the location of the actuators. $\Delta Xvg = X_{cfmin} - Xvg$, $\Delta\tau$ is the skin friction variation $\tau - \tau_0$ due to the actuation. As the skin friction is varying spanwise in the actuated flow, the maximum and minimum values are reported. As can be observed, the counter-rotating configuration is more efficient. It brings a significant skin friction improvement with geometrical parameters which are not far from those of Lin (1999).

The slotted jets have not been studied very much in the literature and most often they were pitched (Zhang (1996, 1997, 2000ab), Akanni & Henry (1995), Vronsky (2000)). The present optimization was based on the previous study by Bernard et al (2000). The actuators location was fixed at $X_d = 17.55$ m. They were set in the counter-rotating configuration. The slot length l was kept fixed at 15 mm. The width e , angle β , spacing inside one device L , spacing between two devices λ and jet velocity V_j were varied (see figure 3). Table 2 gives the optimal configuration obtained. As can be observed, the slotted devices, even with a high velocity ratio (V_j/V_∞), are much less efficient than the passive devices.

The round jets have been the subject of much more studies in the literature (Lin (1990), Selby (1992), Johnston & Nishi (1990), McManus et al (1994)), and were demonstrated by several authors as efficient vortex generators. However, no really quantitative comparison has been performed yet with passive devices. The actuators location was the same as for the slotted jets ($X_d = 17.55$ m). They were studied in both co- and counter-rotating configurations. N_j is the number of holes and Φ the diameter of the holes. Two values of $\Phi = 4$ and 6 mm were used for these tests. Apart for the transverse

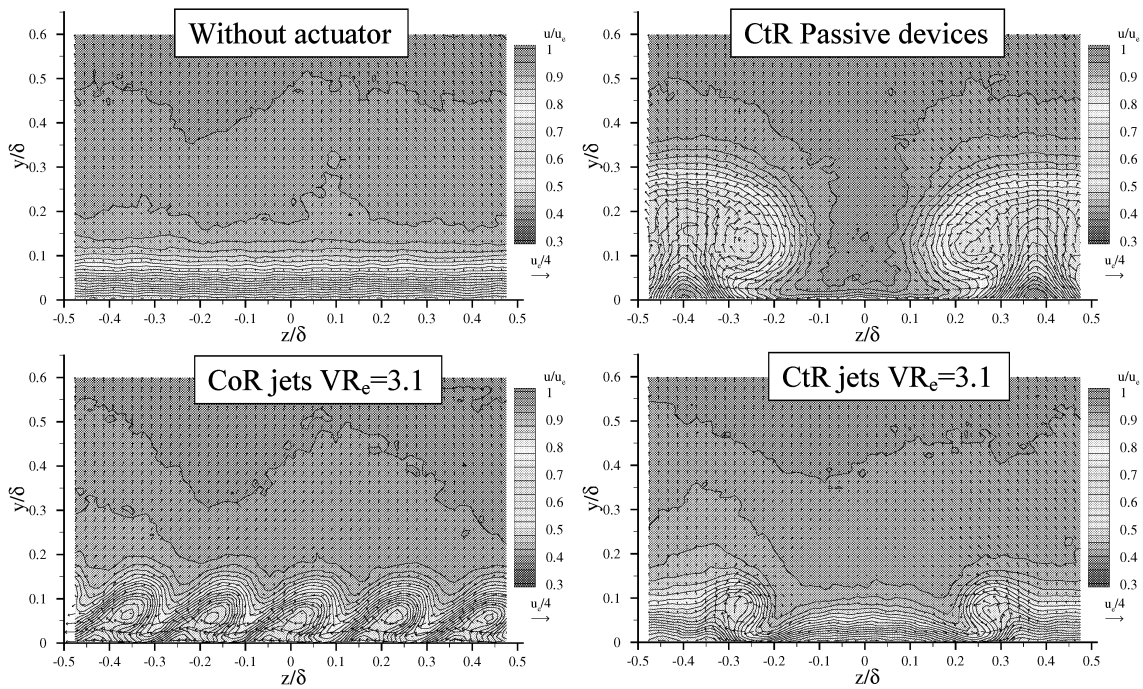


Figure 5 : Mean velocity maps at $\Delta Xd = 0.12$ m for the smooth wall and the three types of actuators tested.

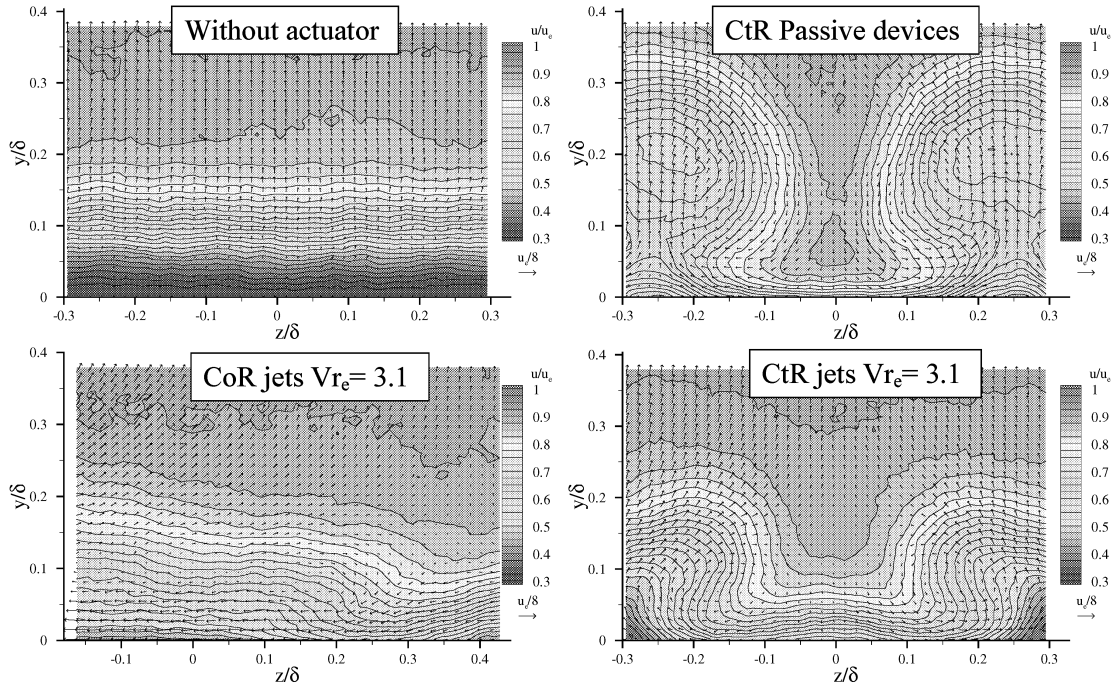


Figure 6: Mean velocity maps at $\Delta Xd = 0.54$ m for the smooth wall and the three types of actuators tested.

spacing, the other parameters are comparable to the passive devices VGs tests. Co-rotating jets tests were performed with $\alpha = 45^\circ$ and 90° , keeping $\beta = 45^\circ$. For the counter-rotating system, the angles were $\alpha = \pm 45^\circ$, $\pm 90^\circ$ and $\pm 135^\circ$, again with $\beta = 45^\circ$. Table 3 gives the results of the optimization procedure for the two

configurations. Both configurations are of comparable efficiency and comparable to the counter-rotating passive devices.

PIV

Based on the optimization results, the counter-rotating passive configuration and the two round jets

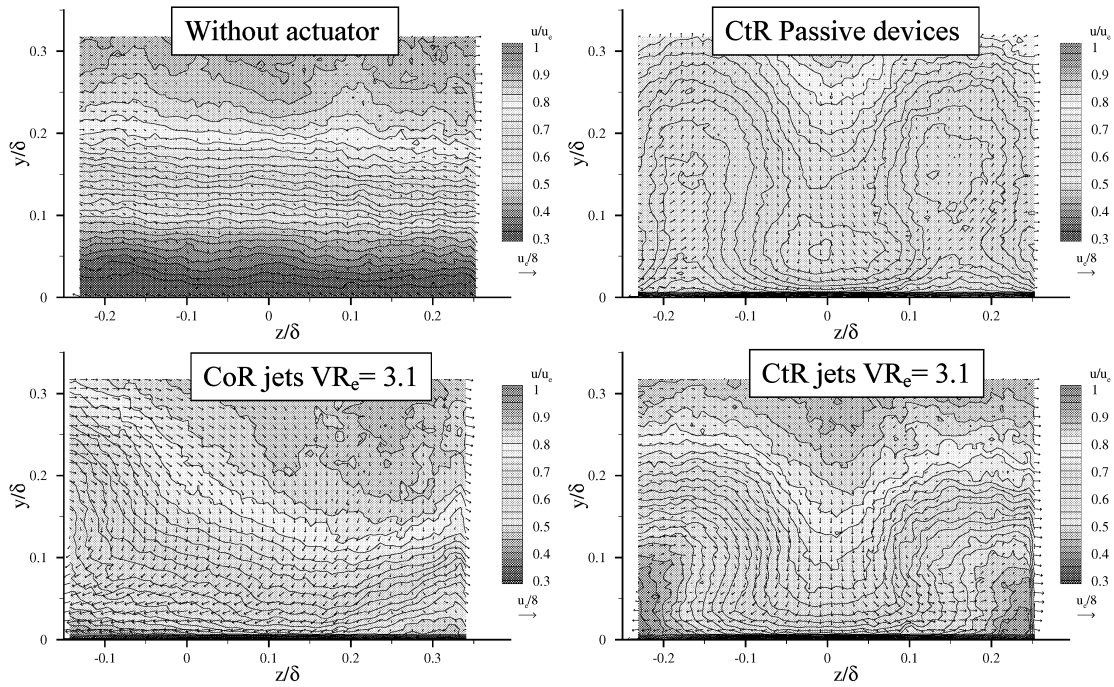


Figure 7: Mean velocity maps at $\Delta X_d = 1.02$ m for the smooth wall and the three types of actuators tested.

configurations were retained for further study using PIV. Measurements were performed at three locations along the bump : $X = 17.67$ m, 18.09 m, 18.57 m, for the three optimal actuators configurations and for the case without actuation. A total of 200 instantaneous velocity maps were recorded for each case and at each station. Figures 5 to 7 show the mean velocity maps obtained by averaging these 200 maps in each plane ($\Delta X_d = X - X_d$). In the first plane (Figure 5), the natural boundary layer is quite thin ($\delta = 70$ mm). The vortices generated by the different types of actuators are clearly visible. The downwash of high momentum fluid toward the wall by the counter-rotating devices is already clearly detectable. It is less evident at this station for the co-rotating devices. The difference in size of the vortices generated by the passive and round jets counter-rotating devices is due to the difference in streamwise location of the two types of actuators ($X_{vg} = 17.10$ m and $X_d = 17.55$ m). Extra tests were performed with the passive devices at the same location as the round jets and the vortices are then of comparable size. Finally, it is interesting to note that the low streamwise momentum fluid is concentrated in the core of the streamwise vortices.

In the second plane (Figure 6) the thickness of the boundary layer has increased significantly ($\delta = 257$ mm). The flow structure of two counter-rotating configurations has not changed significantly. The vortices have increased in size, but the downwash is still clearly visible between them. The most significant change concerns the co-rotating jets system where the individual vortices have disappeared to merge into a large vortical area which has moved to the left of the field by self induction. This merging is probably due to the fact that a limited number of actuators are set in span (as a difference to the passive devices which were spread all through the wind tunnel span). Consequently, there should be an end effect which pushes the vortices to merge. Nevertheless, the

comparison with the smooth case, clearly shows that the streamwise momentum is significantly increased near the wall.

In the last plane (figure 7), which is at the position of minimum skin friction on the smooth bump, the smooth boundary layer is now very thick ($\delta = 455$ mm) and not very energetic (the shape factor is nearly 1.7). For the passive counter rotating devices, as they are fixed upstream of the active devices, the vortices are less individualized in a region of relatively high streamwise momentum which is now fairly homogeneous transversally. The counter-rotating jets vortices are more visible, as they are generated further downstream. For the co-rotating case, a large single vortex appears located outside the field of view on the left, inducing a clear downwash motion in most of the field of view.

Conclusion

An experiment was conducted in the frame of the European project AEROMEMS II in order to optimize and characterize different types of vortex generators with the purpose of controlling an adverse pressure gradient turbulent boundary layer. A quantitative comparison was performed between passive VGs, slotted and round continuous jets. The results show that the passive and the round jets give comparable results while the slotted jets are much less efficient. For the round jets, both co and counter-rotating configurations give comparable results, while for the passive devices, the counter-rotating configuration is the most effective.

A stereo PIV analysis of the flow behind the best actuators clearly shows the streamwise vortex organization. The flow physics is fairly similar between the two counter-rotating configurations (passive and active). It is completely different for the co-rotating jets for which the co-rotating vortices induced merge rapidly

into a large vortical structure which shows an efficiency comparable to the counter-rotating actuators.

A deeper analysis can be performed by investigating the instantaneous velocity maps. This analysis is under way.

Acknowledgements

The research reported here was undertaken as part of the AEROMEMS II project (Advanced Aerodynamic Flow Control Using MEMS, Contract No G4RD-CT-2002-00748). The AEROMEMS II project is a collaboration between BAE SYSTEMS, Dassault, Airbus Deutschland GmbH, EADS-Military, Snecma, ONERA, DLR, LPMO, Manchester University., LML, Warwick University., TUB, Cranfield University., NTUA, and Auxitrol. The project is funded by the European Union and the project partners

REFERENCES

Akanni, S.D., Henry, F.S., 1995, "Numerical calculations for air jet vortex generators in turbulent boundary layer", *CEAS European Forum on High Lift & Separation Control*, Bath, UK.

Angele, K., 2003, "Experimental studies of turbulent boundary layer separation and control", Thesis, Dept. Mechanics, Royal Institute of Technology, Stockholm.

Bernard, A., Dupont, P., Foucaut, J. M., Stanislas, M., 2000, "Identification and assessment of flow actuation and control strategies", AEROMEMS report FREP/CN18/MS001101.

Bernard, A., Foucaut, J.M. , Dupont, P. , Stanislas, M., 2003, "Decelerating boundary layer : a new scaling and mixing length model", *AIAA Journal* vol 41 n°2, pp 248-255.

Betterton, J.G., Hackett, K.C., Ashill, P.R., Wilson, M.J., Woodcock, I.J., Tilman, C.P., Langan, K.J., 2000, "Laser Doppler Anemometry Investigation on sub Boundary Layer Vortex generators for flow control", *10th Intl. Symp. on Appl. of Laser Tech. to Fluid Mech., Lisbon*.

Jenkins, L., Gorton, S.A., Anders, S., 2002, "Flow control device evaluation for an internal flow with an adverse pressure gradient", *AIAA Paper 2002-0266, 40th AIAA Aerospace Sciences Meeting and Exhibit, Reno*.

Johnston, J.P., Nishi, M., 1990, "Vortex Generator Jets – A Means for Flow Separation Control", *AIAA Journal*, vol 28-6, pp 989-994.

Lin, J.C., Howard, F.G., Bushnell, D.M., 1990, "Investigation of several passive and active methods for turbulent flow separation control", *AIAA paper 90-1598 AIAA 21st Fluid Dynamics, Plasma Dynamics and Lasers Conference*.

Lin, J.C., 1999, "Control of turbulent boundary layer separation using micro-vortex generators", *AIAA Paper 99-3404*.

McManus, K.R., Joshi, P.B., Legner, H.H., Davis, S.J., 1994, "Active Control of Aerodynamic Stall Using Pulsed Jet Actuators", *AIAA paper 94-2218*.

Pauley, W. R., Eaton J.K., 1988, "Experimental study of the development of longitudinal vortex pairs embedded in a turbulent boundary layer", *AIAA Journal* vol 26-7, pp 816-823.

Rao, D.M., Kariya, T.T., 1988, "Boundary-layer submerged vortex generators for separation control – An exploratory study", *Space programs and technologies*, pp. 839-846.

Selby, G.V., Lin, J.C., Howard, F.G., 1992, "Control of Low-Speed Turbulent Separated Flow Using Jet Vortex Generators", *Experiments in Fluids* vol 12, pp 394-400.

Soloff, S.M., Adrian, R.J. and Liu, Z.C., 1997, "Distortion compensation for generalized stereoscopic particle image velocimetry", *Meas. Sci. Technol.*, 8, pp. 1441-1454.

Stanewsky, E., Rosemann, H., 2001, "Active Flow Control Applied to Military and Civil Aircraft", *Symposium of the RTO Applied Vehicle Technology Panel (AVT) Braunschweig, Germany, 8-11 May 2000*.

Vronski, T., 2000, "High performance cost-effective large wind turbine blades using air jet vortex generators", *ETSU report n° W/41/00541*, <http://www.dti.gov.uk/energy/renewables/publications/pdfs/W4100541.pdf>.

Zhang, X., Zhang, H-L, Collins, M.W. , 1996, "Some Aspects of Streamwise Vortex Production Using Air Jets", *AIAA paper 96-020*.

Zhang, X., Collins, M.W., 1997, "Measurements of a longitudinal vortex generated by a rectangular jet in a turbulent boundary layer", *Phys Fluids* vol 9-6, pp.1665-1673.

Zhang, X., 2000a, "An inclined rectangular jet in a turbulent boundary layer-vortex flow", *Experiments in Fluids* vol 28, pp 344-354.

Zhang, X., 2000b, "Turbulence measurements of an inclined rectangular jet embedded in a turbulent boundary layer", *International Journal of Heat and Fluid Flow* vol 21, pp 291-296.